

## USING WASTE FROM PET TO PRODUCE GRAPHENE-BASED ADSORBENT USED FOR DYES REMOVAL FROM AN AQUEOUS SOLUTION

Lenka Blinová, Maroš Sirotiak, Peter Rantuch, Alica Pastierová, Peter Gogola

Faculty of Materials Science and Technology in Trnava  
Slovak University of Technology in Bratislava  
Jana Bottu 2781/25, SK 917 24 Trnava, Slovakia  
lenka.blinova@stuba.sk (L.B.); maros.sirotiak@stuba.sk (M.S.);  
peter.rantuch@stuba.sk (P.R.); alica.pastierova@stuba.sk (A.P.);  
peter.gogola@stuba.sk (P.G.)

Received 07 May 2024  
Accepted 12 August 2024

DOI: 10.59957/jctm.v60.i1.2025.3

---

### ABSTRACT

Polyethylene terephthalate (PET) is the most commonly used thermoplastic polymer around the world. This study aims to create a graphene-based adsorbent from PET waste bottles (PET flakes) and test its effectiveness in removing methylene blue (MB) from aqueous solutions. To produce the adsorbent, the carbonization process of PET flakes was carried out in a closed reaction vessel. The properties of both PET flakes and the synthesized adsorbent were assessed using various techniques including FT-IR, TGA, SEM, EDX, and XRD. Two isotherm models (Langmuir and Freundlich) and two kinetic models (pseudo-first-order and pseudo-second-order) were used to describe the sorption isotherm and kinetics study. The results showed that the graphene-based adsorbent was effective in removing MB from water. To further increase its efficiency, it would be appropriate to functionalize its surface or adjust the preparation procedure.

*Keywords:* PET, carbonization, graphene-based adsorbent, adsorption, methylene blue.

---

### INTRODUCTION

Dyes are synthetic organic compounds that are widely used in various industries, such as printing, pharmaceuticals, food, cosmetics, leather, and textiles. Each type of dye has distinct qualities, benefits, and drawbacks of its own, and depending on those qualities, it is employed for particular purposes [1]. The dyes can be harmful to the aquatic flora, aquatic life and also to human beings [2, 3] if their use and disposal are not managed in an environmentally sustainable way [4].

Methylene Blue, also known as Methylthionium chloride, Swiss Blue, Urolene Blue, and other names, is an organic chloride salt that is used both as a dye and a medication [5]. It is one of the oldest organic dyes and is frequently used as a cationic dye in synthetic

processes [6]. MB dye is commonly used in the apparel and textile industries to dye materials, as well as in the leather and paper industries. Additionally, significant amounts of MB dye are utilized in the food, cosmetic, and pharmaceutical industries. MB is also used in both human and veterinary medicine for various therapeutic and diagnostic purposes. These applications include the use MB as a bacteriological stain, as a redox colourimetric agent, as a melanoma targeted agent, as an antihaemoglobinaemic, as an antidote, and as an antiseptic. It is also used as a disinfectant, biological stain, in pH and redox indicator reagents, and analytical chemistry is utilized to determine anionic surfactants [7].

Even though MB is important for many different fields, its presence can seriously endanger both human health and the environment [4, 8].

For example, it causes aesthetic damage to the water bodies and the significant natural problem of it is the absorption and reflection of sunlight into water [2]. This can influence the rate of photosynthesis and level of dissolved oxygen which impacts the entire aquatic biota [9].

MB is toxic above a certain concentration, carcinogenic, and environmentally persistent [10]. At therapeutic doses of less than 2 mg kg<sup>-1</sup>, MB is a safe medication [11]. The combination of MB with medication that either boosts or contains serotonin has the potential to be fatal. At doses greater than 5 mg kg<sup>-1</sup>, the monoamine oxidase inhibitory characteristics of MB can induce fatal serotonin toxicity [4, 11]. Teratogenic and embryotoxic MB were confirmed in an exposure study of MB to angelfish and rat, respectively [4]. Because MB might decrease renal blood flow, it is important to use caution when administering it to individuals with renal failure [11]. MB also causes for example breathing difficulties, blindness, digestive and mental disorders, nausea, diarrhoea, vomiting, cyanosis, shock, gastritis, jaundice, methemoglobinemia, skin redness and itching, skin necrosis, increased heart rate [4, 10].

Adsorption is a cost-effective method that can be used to remove colours from contaminated water. This method has several advantages, including lower costs compared to other processes (provided that the adsorbent is cheap), the availability of natural adsorbents, ease of operation, high efficiency, and insensitivity to harmful elements [4]. Factors which affect adsorption include pH of solution, contaminants in solution, initial dye concentration, adsorbent weight, particle size and surface area, temperature, stirring speed, pressure, properties of the adsorbent, contaminant properties and activation of solid sorbent [12]. A lot of adsorbents can be used for dyes removal from wastewater. They include uses of activated carbon (commercial activated carbon, activated carbon from waste materials), non-conventional (natural and synthetic clay, bio-adsorbents, agricultural waste, industrial waste), hybrid nanomaterial (natural and synthetic clay-based, fly ash based, bio-adsorbents based, carbon-based, activated carbon-based, carbon nanotube-based, graphene and reduced graphene oxide), metal oxide-based hybrid materials (magnetic metal oxide, nanomagnetic metal-oxide), metal-organic frameworks, polymers and their nanocomposites (chitosan-based, miscellaneous polymer-based, pure

polyaniline and polypyrrole, polyaniline and polypyrrole nanocomposites) [13].

With its properties (e.g., high strength, high rigidity and hardness, very low moisture absorption, good creep resistance, good chemical resistance against acids, good adhesion and welding ability [14]), PET has become an essential material in many applications. The growing use of PET and the incorrect way of its disposal have caused significant damage to the environment and to human health [15]. Because of this, the disposal of PET waste represents a significant worldwide problem. Among the most popular ways of disposing of PET waste can include burning with recovering energy, chemical recycling or recycling feedstock to create carbon-enriched materials and gaseous and liquid products [16]. However, PET waste recycling brings with it various limitations. The used materials' structure remains mostly unchanged, but the recycled raw materials' quality declines (recycled PET is often not as strong or durable as virgin PET [17]), and, accordingly, the range of further use is reduced [15]. The recycling process of PET is also energy-intensive, which means that it contributes to greenhouse gas emissions [17]. The release of heat and volatile compounds is a negative impact of the burning process of PET [16]. Another way of processing PET waste is to produce an eco-friendly graphene-based adsorbent by carbonization process. This material can be consequently used for example to remove MB from wastewater. Due to the hazardous properties of MB and the negative of PET recycling process, this way of using PET waste is a good alternative.

The goal of this manuscript is to use waste materials, specifically PET bottle waste, to create a graphene-based adsorbent. The efficiency of this material in removing cationic dye MB was tested to evaluate its sorption properties and adsorption capacity. The preparation process for the graphene-based adsorbent is a simple and repeatable one. It involves the thermal decomposition of PET waste in a closed system under autogenic pressure.

## **EXPERIMENTAL**

### **Sorbate**

Methylene blue (MB) was obtained from Mikrochem. It was used as contaminant in this study. The dye solution which simulates the contaminated water has been prepared by dissolving MB in distilled water without

further purification to obtain a desired concentration. Other dye concentrations used in this study were obtained by dilution processes. The pH of the dye solutions was not adjusted. All used reagents were commercially available and used without additionally purification.

### Sorbent

The PET flakes used in this study were obtained from the General Plastic Joint Stock Company in Slovakia. These flakes are the final product of PET bottle recycling. We used hot washed and chemically cleaned PET flakes in various shades of blue as the raw material for producing graphene-based adsorbent. This adsorbent was then used to remove dyes from wastewater.

Graphene-based adsorbents were produced by carbonizing PET flakes under predetermined thermal conditions in a closed reaction vessel (Fig. 1). The same process for the production of graphene-based material were also used from El Essawy et al. [16] and Ezzat et al. [18]. PET flakes (various blue pieces of PET flakes labelled as A, B, C; dimension of width, height, thickness in range 0.16 - 20 mm) were introduced into reaction vessel, then the closed reaction vessel was inserted inside the electric furnace. The reaction vessel was made of stainless austenitic chrome-nickel-molybdenum steel (1.4401). Electric furnace model Nabertherm 24/11/P330 (maximum control temperature 1100°C) was used for thermal preparation of graphene. The furnace was heated to a temperature of 800°C with a heating rate of 8°C per min. The temperature of 800°C was held for 1 hour and after this time the system was allowed to cool.

The resulting product was collected, crushed, and stored in a closed container.

### Sorption experiment

The sorption was each times realized using batch experiments under different conditions. Prior to initiating the sorption experiment, a calibration curve was created with known MB concentration (1.0 - 12.5 mg L<sup>-1</sup>). All the samples including a blank were placed in Agilent Cary 60 UV-Vis spectrophotometer. The corresponding absorbance at 664 nanometres was recorded.

For the kinetic experiments, 5.0 mL of MB solution with concentration of 10.0 mg L<sup>-1</sup> were added to separate glass vials containing 5.0 mg of adsorbent. The amount of adsorbent dosage and dosage of MB solution was determined based on preliminary experiments. The mixture was then shaken for different time limit (0 - 6 h) at room temperature using a rotary shaker RSLAB1 at a constant rotation speed of 50 rpm. After the kinetic experiments, the graphene-based adsorbent was removed using centrifugation (1200 rpm) and the residual concentration of MB in pure supernatant solution was determined.

Equilibrium isotherm experiments were carried out at room temperature for different concentrations of MB 2.5, 5.0, 7.5, 10.0 and 12.5 mg L<sup>-1</sup> using 5.0 mg of sorbent. The mixture was then shaken for 6 hr at room temperature and the samples were handled as in the previous case.

All of sorption experiment was repeated three times, and the results obtained were averaged.

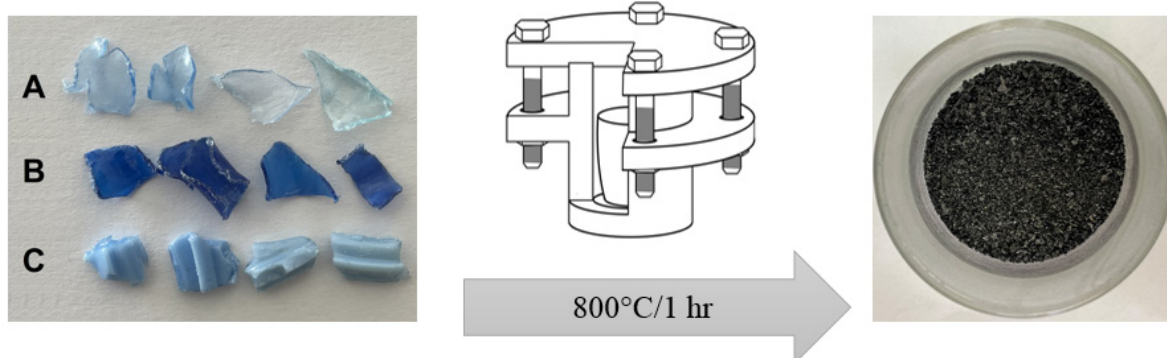


Fig. 1. Cleaned PET flakes before and after carbonization process.

### Sorption data analyses

The removal efficiency of MB on the graphene-based adsorbent, % can be calculated [19]:

$$RE = \frac{(C_0 - C_e) \times 100}{C_0} \quad (1)$$

where,  $C_0$  is the initial concentration of dye,  $\text{mg L}^{-1}$ ;  $C_e$  is the equilibrium concentration of dye after treatment,  $\text{mg L}^{-1}$ . The equilibrium adsorption capacity of MB on the graphene-based adsorbent  $Q_e$ ,  $\text{mg g}^{-1}$  was calculating using the mass balance equation [19]:

$$Q_e = \frac{(C_0 - C_e) \times V}{m} \quad (2)$$

where,  $V$  is the volume of MB solution,  $L$ ; and  $m$  is the weight of adsorbent,  $g$ .

Adsorption kinetics described the solute uptake rate. This rate controls the residence time of adsorbate uptake at the solid-solution interface. The most common models used for adsorption kinetics are the Pseudo-first order and Pseudo-second order kinetics model. Pseudo-first order is mathematically expressed as follow [20]:

$$\left(\frac{dQ_t}{dt}\right) = k_1 \times (Q_e - Q_t) \quad (3)$$

or linear form:

$$\log(Q_e - Q_t) = \log Q_e - k_1 \times t \quad (4)$$

where,  $Q_e$  is the amount of MB sorbed at equilibrium,  $\text{mg g}^{-1}$ ;  $k_1$  is the rate constant of Pseudo-first order adsorption,  $\text{min}^{-1}$  and  $Q_t$  is the quantity of MB sorbed at time,  $\text{mg g}^{-1}$ . The pseudo-first-order model describes the rate of adsorption which is proportional to number of unoccupied binding sites on adsorbents [21]. Pseudo-second order equation is based on adsorption equilibrium capacity can be expressed as [22]:

$$\left(\frac{dQ_t}{dt}\right) = k_2 \times (Q_e - Q_t)^2 \quad (5)$$

or linear form:

$$\frac{t}{Q_e} = \left(\frac{1}{k_2 \times Q_e^2}\right) + \left(\frac{t}{Q_e}\right) \quad (6)$$

where,  $k_2$  is the rate constant of Pseudo-second order adsorption,  $\text{g mg}^{-1} \text{min}^{-1}$ . The pseudo-second-order kinetic model describes the adsorption of adsorbates onto

adsorbents where the chemical bonding (interaction) between adsorbates and functional groups on the surface of adsorbents are responsible for the adsorption capacity of adsorbent. It is based on equilibrium adsorption, which is dependent on the amount of adsorbate adsorbed onto the surface of an adsorbent and the amount of adsorbate adsorbed at equilibrium [23].

Adsorption isotherm models are mathematical equations that describe the relationship between the amount of sorbate adsorbed on an adsorbent and the concentration of sorbate in solution when equilibrium has been reached at constant temperature. Langmuir model implies that the energies of sorption onto the surface are homogeneous and can be expressed as follow:

$$Q_e = \frac{Q_{\max} \times K_L \times C_e}{1 + K_L \times C_e} \quad (7)$$

or linear form:

$$\frac{C_e}{Q_e} = \frac{C_e}{Q_{\max}} + \frac{1}{K_L \times Q_{\max}} \quad (8)$$

where,  $K_L$  is the constant of the free energy of sorption,  $L \text{ mg}^{-1}$ , and  $Q_{\max}$  is the maximum sorption capacity,  $\text{mg g}^{-1}$ . Langmuir's isotherm was used for monolayer adsorption on a surface containing a finite number of identified sites with negligible interaction between adsorbed molecules and assumes uniform energies of adsorption on the surface. In addition, the maximum adsorption depends on the saturation level of monolayer [24]. The Langmuir isotherm also can be articulate as dimensionless constant separation factor  $R_L$  [25]:

$$R_L = \frac{1}{1 + Q_{\max} \times C_0} \quad (9)$$

where,  $C_0$  is the highest dye concentration,  $\text{mg L}^{-1}$ , the values of  $R_L$  the types of isotherms whereby when  $R_L > 1$ , the adsorption is unfavourable, linear when  $R_L = 1$ , favourable when  $0 < R_L < 1$  or irreversible when  $R_L = 0$ . The Freundlich equation is basically empirical but is often useful as a means for data description and representing the equilibrium on heterogeneous surfaces and does not assume monolayer coverage. Freundlich model can be represented by using the following equation:

$$Q_e = K_F \cdot x (C_e)^{1/n} \quad (10)$$

or linear form:

$$\log Q_e = \log K_F + \frac{1}{n} \times \log C_e \quad (11)$$

where,  $K_F$  is Freundlich sorption coefficient,  $\text{mg g}^{-1}$ ; and  $n$ ,  $\text{L mg}^{-1}$  is an empirical coefficient that indicates the sorption intensity. In general, if this empirical coefficient is greater than 1, that means adsorbate is favourably adsorbed on the adsorbent whereas if is lower than 1, that illustrates the adsorption process is chemical in nature [24].

All of calculations was realized using Microsoft Excel 2016 software. The suitability of applying the pseudo-first or pseudo-second order model, as well as the suitability of the Freundlich or Langmuir isotherm model, was determined by evaluating the calculated correlation coefficients.

### Characterization of PET flakes and produced graphene-based adsorbent

The characteristics of PET flakes and the produced graphene-based adsorbent were carried out by the following methods: Fourier transform infrared spectroscopy – attenuated total reflectance (FTIR ATR), Thermogravimetric analysis (TGA), Scanning electron microscopy (SEM), Energy dispersive X-ray (EDX) analysis, and X-ray diffraction (XRD) analysis.

#### FT-IR ATR

For identification and verification of functional groups present in input material (Fig. 1, various blue pieces of PET flakes labelled as A, B, C) used for produce graphene-based adsorbent was used FT-IR ATR analysis. For this analysis, Varian FT-IR Spectrometer 660 from Agilent Technologies, Inc., located in Santa Clara, CA, USA was used. The specimens were directly applied on a diamond crystal of the ATR accessory known as GladiATR (PIKE Technology Inc., Madison, WI, USA). The resulting spectra underwent correction to account for air absorbance in the background. These spectra were recorded using a Varian Resolutions Pro instrument and involved measurements within the 4000 - 400  $\text{cm}^{-1}$  range, each spectrum was measured 256 times at resolution 4.

#### TGA

Thermogravimetric analysis (TGA) of graphene-based adsorbent was performed on a Netzsch STA 449 F5 Jupiter device. It was carried out in a stream of a mixture of nitrogen and oxygen simulating air (80 %  $\text{N}_2$  + 20 %  $\text{O}_2$ ) at a flow rate of 60  $\text{mL min}^{-1}$ . The weight of the sample was 4.9633 mg and the heating rate was set to 10  $^{\circ}\text{C min}^{-1}$ . The maximum temperature during the measurement was set to 1000  $^{\circ}\text{C}$ .

#### SEM

SEM was used to document the morphology graphene-based adsorbent particles. A JEOL JSM 7600F scanning electron microscope equipped with a Schottky field emission electron source (SEM, Jeol Ltd., Tokyo, Japan) was utilised. The imaging was done using a back scattered electron imaging detector (detector BSE-SM-74280RBEI in composition mode).

#### EDX

The local elemental composition of the graphene-based adsorbent particles was measured with an Oxford Instruments X-Max silicon drift detector, energy dispersive X-ray spectrometer (EDS, Oxford Instruments plc, Abingdon, United Kingdom) attached directly to the SEM.

#### XRD

The semi-crystalline nature of the sample was shown by recording its XRD pattern via a PANalytical Empyrean X-ray diffractometer (XRD) (Malvern Panalytical Ltd., Malvern, United Kingdom). The measurements were performed in Bragg-Brentano geometry. Theta-2Theta angle range between 10  $^{\circ}$  and 130  $^{\circ}$  2Theta was chosen. The Cu anode XRD source was set to 40 kV and 40 mA. The incident beam was modified by 0.04 rad sollar slit, 1/4  $^{\circ}$  divergence slit and 1/2  $^{\circ}$  anti-scatter slit. The diffracted beam path was equipped with a 1/2  $^{\circ}$  anti-scatter slit, 0.04 rad sollar slit, Ni beta filter and PIXcel3D position sensitive detector operated in 1D scanning mode. The phase quality was analysed using PANalytical Xpert High Score program (HighScore Plus version 3.0.5) with the ICSD FIZ Karlsruhe database.

## RESULTS AND DISCUSSION

### FT-IR ATR results

The characteristic bands of the PET material appear in all 3 types of PET flakes (various blue pieces of PET flakes) which are contained in input material used for

graphene-based adsorbent production. This analysis was made for verification type of plastic of input material. As we can see in Fig. 2, the absorption bands of sample A were observed at 2965 and 2904  $\text{cm}^{-1}$  (C-H, symmetrical stretching, peak 1 and 2 respectively), 1710  $\text{cm}^{-1}$  (stretching of C=O of carboxylic ester group, peak 3), 1578, 1506, and 1406  $\text{cm}^{-1}$  (aromatic skeleton stretching, peak 4, 5, 6 respectively), 1453 and 870  $\text{cm}^{-1}$  ( $\text{CH}_2$  bending and  $\text{CH}_2$  rocking, peak 7 and 8 respectively), 1237 and 1091  $\text{cm}^{-1}$  (C-C-O stretching of ester group, peak 9 and 10 respectively), 1015 and 720  $\text{cm}^{-1}$  (in-plane C-H stretching and out-of-plane C-H bending of aromatic ring, peak 11 and 12 respectively). The wavenumber values for PET are consistent with the results of other authors [26 - 28]. The specific wavenumbers values in the previous description apply to sample A, however, it can be seen from the figure that the peaks for other samples (B, C) are at almost identical wavenumbers. That means that all pieces (A, B, C) are PET material.

### TGA result

The thermogravimetric curve (Fig. 3) of the graphene-based adsorbent in air indicates the stability of the sample up to a temperature of approximately 445°C. It is followed by decomposition in a single stage, which is practically complete at 625°C. The maximum rate of weight loss was recorded at 588°C. The rest at 1000°C represents 0.5 %.

According to Farivar et al. is the maximum DTG for graphene oxide according to its size particles in the temperature range of 560 - 616°C, in the case of graphene it occurs between 650 - 713°C and in the case of graphite from 840 to 950°C [29]. Considering the measured maximum, the produced material therefore falls into the area of graphene oxide. The lower temperature of the DTG maximum in the case of graphene oxide compared to graphene is according to Farivar et al. caused by the fact that less heat energy is required to overcome weaker nongraphitic  $\text{sp}^3$  hybridized carbon with a high density of defects after the rigorous oxidation reaction compared

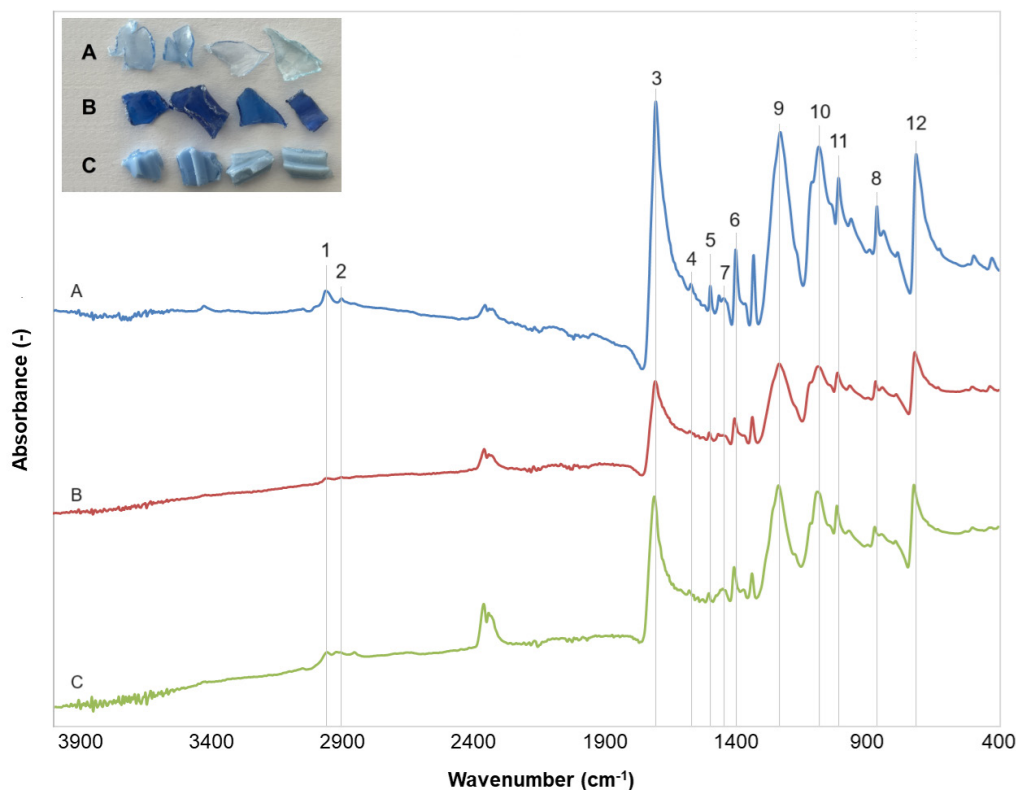


Fig. 2. FT-IR ATR spectra of PET flakes.

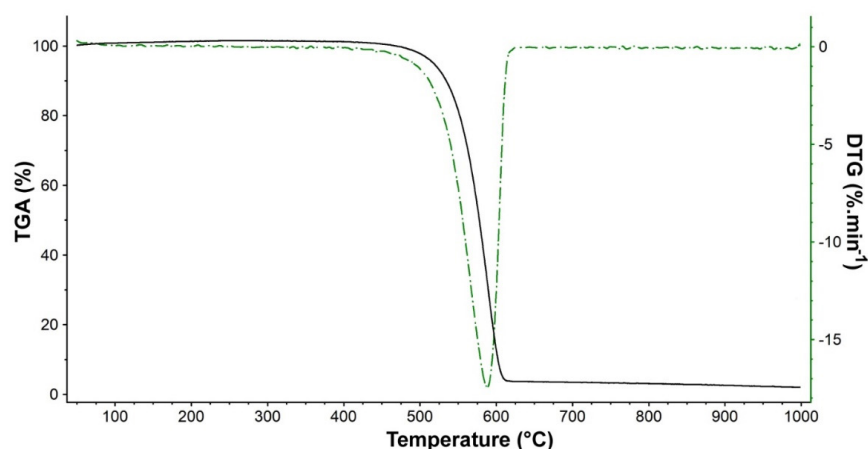


Fig. 3. Thermogravimetric analysis of produced graphene-based adsorbent in air.

with graphene and graphite [29].

In the case of graphene oxide, Yap et al. describe decomposition in several stages. Up to a temperature of 110°C, mass loss occurs due to the removal of moisture, in the next step (with the maximum rate of mass loss at 190°C), oxygen containing functional groups are removed, and finally, around a temperature of 538°C, pyrolysis of carbon skeleton occurs [30]. Thermogravimetric measurements of graphene-based adsorbent made from recycled PET do not show the first two stages of decomposition. While the negligible moisture content is probably due to the prevention of moisture access to the samples, the absence of the second stage indicates a very low content of oxygen groups. Such a TG and DTG curve is described for reduced graphene oxide [31]. The measured results thus indicate that the obtained material shows defects in the graphene structure and should be further referred to as reduced graphene oxide.

### SEM, EDX and XRD results of the prepared graphene-based adsorbent

To obtain the surface morphology of the prepared graphene-based adsorbent, the analysis of SEM was used (Fig. 4). The morphology of this adsorbent, seen in Fig. 4a, is heterogeneous, rough, and uneven, with many tiny holes dispersed erratically throughout the surface (Fig. 4b).

SEM/EDX chemical composition measurements revealed that the samples are composed on average

mainly of C and O as expected [16, 18]. Nevertheless, impurities with an increased content of Fe, Cr, Mn and Ni can be identified via targeted point measurements of random particles (Fig. 5, Table 1). Presence of these impurities can be explained by the use of a stainless-steel based crucible. The reaction vessel is unavoidably damaged during the production process forming tiny sub-micron metallic particles. These particles oxidised and can be traced back sticking to the graphene particles themselves (points 1 and 2 in Fig. 5, Table 1). Different literature sources indicate a range of impurities like Cu, Al and Si identified in their graphene samples. These can be related to their respective production procedure and quality (purity) of the starting material [16, 18].

The recorded XRD pattern has three distinct peaks as shown in Fig. 6. All three peaks are very broad indicating a disordered, amorphous-like atomic structure. For all of them, one can conclude that they represent a range of d-spacing distances instead of a single value as usual for crystalline materials. As indicated by multiple literature sources [16, 18, 32 - 35] all three peaks can be attributed to a selected set of crystallographic planes of graphite (ICSD Database, PDF 00-001-0646). The first peak (C1) at approx. 22° 2Theta can be correlated to the (002) plane of crystalline graphite. It refers to a range of interlayer distances (c-lattice parameter of the hexagonal lattice) which are on average larger than those in crystalline graphite (approx. 0.76 nm vs. 0.68 nm). The second peak (C2) at approx. 43.5° is additionally rather asymmetric, as it is the sum of multiple peaks, most notably from

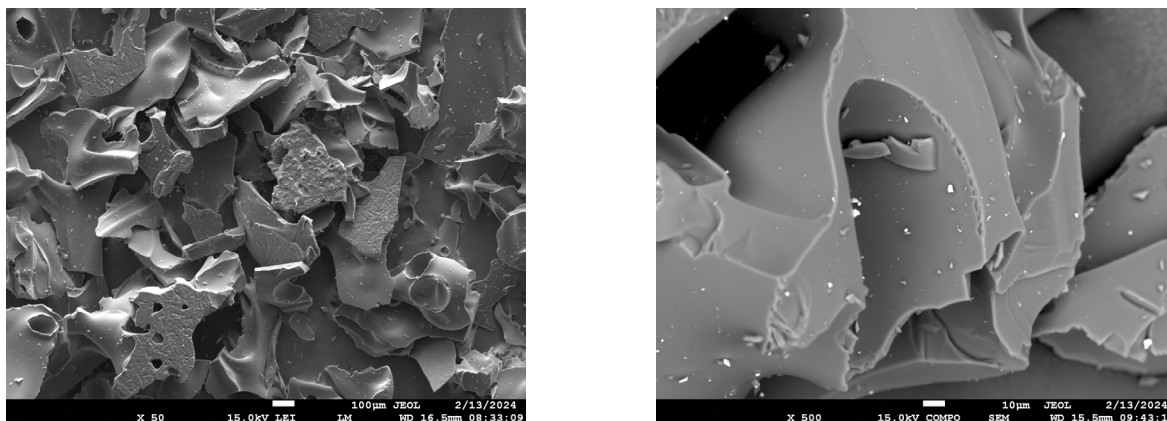


Fig. 4. SEM images of the prepared graphene-based adsorbent.

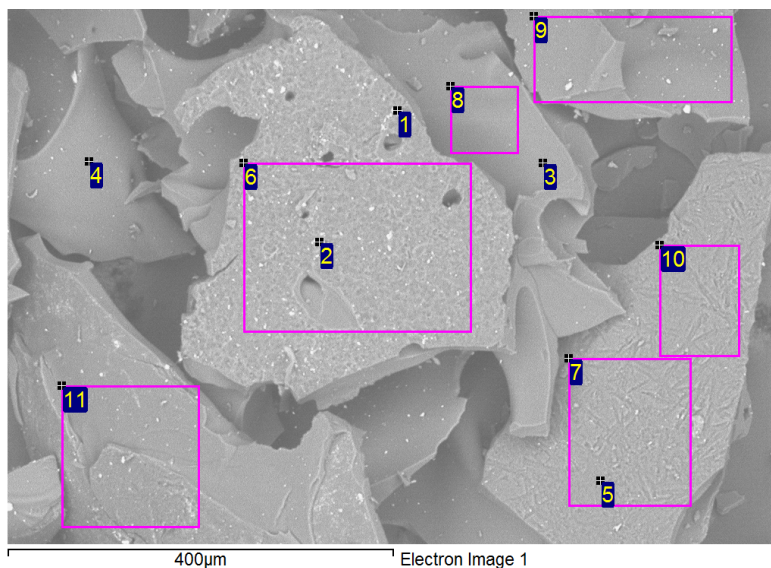


Fig. 5. SEM image of the prepared graphene-based adsorbent including sites of EDX point measurements.

the planes (100) and (101). These are linked mainly to the a-lattice parameter of graphite. The third peak centred around  $80^{\circ} 2\theta$  can be mainly attributed to the (110) and (112) crystallographic planes. The centre positions of C2 and C3 indicate that the a-lattice parameter of our sample is comparable to hexagonal graphite at approx. 0.243 nm.

#### Sorption kinetics and sorption isotherms

In Fig. 7, we can see how the removal efficiency of MB by a graphene-based adsorbent at room temperature is affected by the contact time. The results show that the efficiency of dye removal increased as the contact time

increased. The sorption rate was fast at the beginning and gradually slowed down over time. This could be due to the decreasing number of active sites on the graphene surface. The polar functional groups on the surface of the graphene help adsorb water through hydrogen bonds, while the anionic dye molecules experience coulombic repulsion with the oxygen-containing functional groups (such as carbonyl and carboxyl) present on the graphene surface [36]. The experimental data shows that after 4 h of contact time, 35.4 % of MB was removed.

The kinetics data was correlated using two models - Pseudo-first (Fig. 8a) and Pseudo-second (Fig. 8b). The

Table 1. Chemical composition of the prepared graphene-based adsorbent as measured by EDX on sites indicated in Fig. 5.

| Site    | Measurement type | C    | O    | Cr   | Mn  | Fe   | Ni  | Total | Comment                               |
|---------|------------------|------|------|------|-----|------|-----|-------|---------------------------------------|
| wt.%    |                  |      |      |      |     |      |     |       |                                       |
| 1       | point            | 25.6 | 30.4 | 20.9 | 3.2 | 18.6 | 1.4 | 100   | metallic particle                     |
| 2       | point            | 51.2 | 20.3 | 0.7  | -   | 27.8 | -   | 100   | metallic particle                     |
| 3       | point            | 89.9 | 10.1 | -    | -   | 0.0  | -   | 100   | -                                     |
| 4       | point            | 95.0 | 5.0  | -    | -   | 0.0  | -   | 100   | -                                     |
| 5       | point            | 92.9 | 7.2  | -    | -   | 0.0  | -   | 100   | -                                     |
| 6       | area             | 86.9 | 12.4 | -    | -   | 0.7  | -   | 100   | -                                     |
| 7       | area             | 91.3 | 8.7  | -    | -   | 0.0  | -   | 100   | -                                     |
| 8       | area             | 88.4 | 11.6 | -    | -   | 0.0  | -   | 100   | -                                     |
| 9       | area             | 88.6 | 11.4 | -    | -   | 0.0  | -   | 100   | -                                     |
| 10      | area             | 91.1 | 8.9  | -    | -   | 0.0  | -   | 100   | -                                     |
| 11      | area             | 92.2 | 7.8  | -    | -   | 0.0  | -   | 100   | -                                     |
| average |                  | 90.7 | 9.2  | -    | -   | 0.1  | -   | 100   | average - metallic particles excluded |
| stdev   |                  | 2.5  | 2.4  | -    | -   | 0.2  | -   | -     |                                       |

experimentally obtained values were found to be better described by the Pseudo-second model, with constants  $k_2$  constant  $6.60 \times 10^{-3} \text{ g mg}^{-1} \text{ min}^{-1}$  and  $Q_e$   $4.32 \text{ mg g}^{-1}$ . The accuracy is  $R^2 = 0.9887$ . However, the kinetic data can also be well described by the Pseudo-first model with the  $k_1$  constant  $7.98 \times 10^{-3} \text{ L min}^{-1}$  and  $Q_e$   $3.98 \text{ mg g}^{-1}$ , and the accuracy is  $R^2 = 0.9649$ . The slightly better fit of the Pseudo-second order model indicates a slight influence of sorption by functional groups on the graphene-based adsorbent surface.

The experimental data for sorption were fitted with Langmuir (Fig. 9a) and Freundlich (Fig. 9b) models. The Langmuir isotherm had parameters  $K_L = 1.59 \text{ L mg}^{-1}$  and  $Q_{\text{max}} = 4.66 \text{ mg g}^{-1}$ , while the Freundlich isotherm had parameters  $K_F = 2.70 \text{ mg g}^{-1}$  and  $n = 3.96 \text{ L mg}^{-1}$ . The Freundlich model gave a higher coefficient of determination ( $R^2 = 0.9926$ ) compared to the Langmuir model ( $R^2 = 0.9811$ ), indicating that it was a more appropriate model for representing the sorption data. The Freundlich empirical coefficient  $n$  was greater than 1, suggesting favourable adsorption, meaning that as the solute concentration increased, the amount adsorbed also increased at an increasing rate. The Langmuir constant separation factor  $R_L = 0.017$  is favourable for adsorption ( $0 < R_L < 1$ ) and due to its very low value, approaches an irreversible event (when  $R_L = 0$ ).

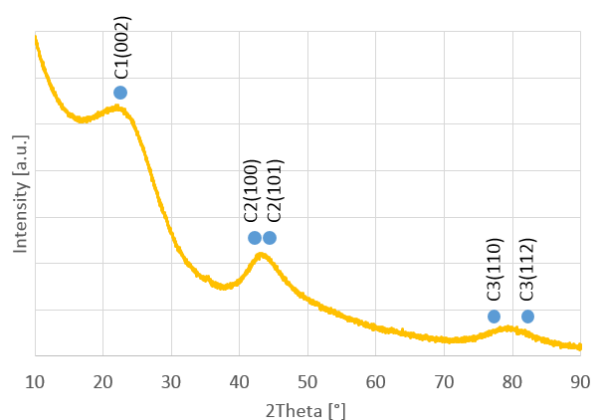


Fig. 6. XRD pattern of the prepared graphene-based adsorbent.

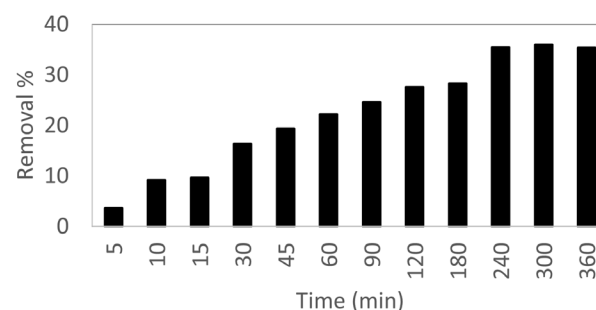
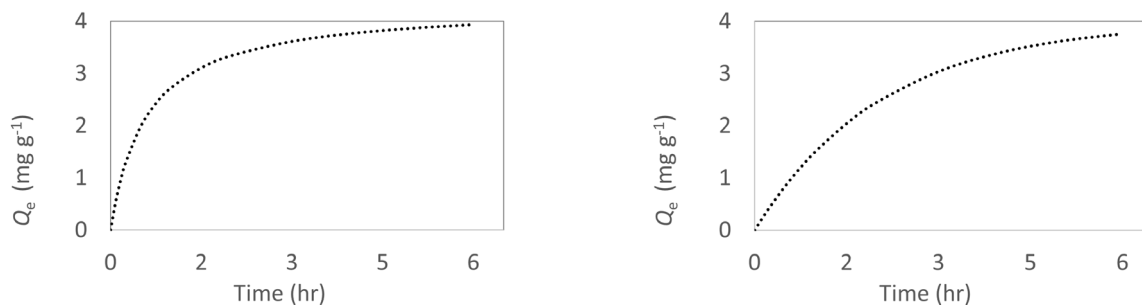


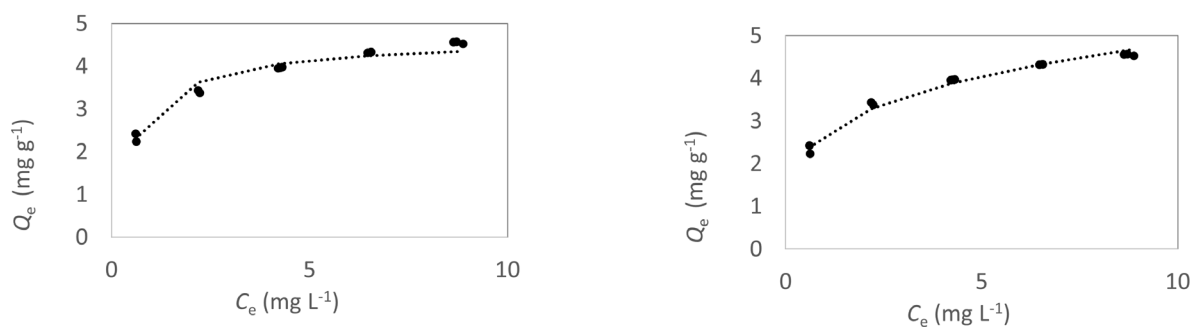
Fig. 7. Removal efficiency of MB by graphene-based adsorbent.



a)

b)

Fig. 8. Pseudo-first and Pseudo-second order fitted kinetic data.



a)

b)

Fig. 9. Experimental data fitted by Langmuir and Freundlich isotherms.

## CONCLUSIONS

PET is the most frequently utilised thermoplastic polymer worldwide which is used to make single-use beverage bottles, packaging, and clothing, and it is one of the largest sources of plastic waste. That's why we use this in our study this material for prepare graphene-based adsorbent as a potential sorbent for dye removal.

This work involved the preparation of graphene-based adsorbent via the carbonization process of PET flakes under predetermined thermal conditions in a closed reaction vessel.

The graphene-based adsorbent was observed to form randomly shaped flat particles. Its chemical composition consisted mainly of carbon, with an average of 9 wt.% oxygen. During the targeted point analysis of selected particles, metal oxide impurities were identified. The XRD pattern was similar to that of graphite; however, the crystal lattice parameters „a“ and „c“ varied significantly, leading to broad peaks.

The results of the thermogravimetric analysis show

that the graphene-based adsorbent obtained from PET is thermally stable in oxygen up to 445°C and subsequently decomposes in one step. Based on the obtained measurements, it can be concluded that the material produced can be classified as reduced graphene oxide.

Based on the experimental sorption data, it was observed that 35.4 % of methylene blue was removed in 4 h. The sorption kinetics analysis showed that the Pseudo-second order model was more accurate in representing the experimental data ( $R^2 = 0.9887$ ). Additionally, the experimental results demonstrated that the sorption data for methylene blue dye can be represented by the Freundlich isotherm model with an  $R^2$  value of 0.9926. The Freundlich empirical coefficient indicated favourable adsorption, while the Langmuir constant separation factor suggested irreversible adsorption.

Our study indicates that the graphene-based adsorbent developed by us is a viable substitute for other sorption materials. Its primary advantage is that it uses waste PET for its preparation, making

it an economical adsorbent. However, to further enhance its sorption capacity, it is recommended to consider functionalizing its surface. This would help in improving the effectiveness of the adsorbent in removing contaminants from water. Additionally, it is possible to modify the preparation procedure of the graphene-based adsorbent.

### **Acknowledgments**

*This work was supported by the VEGA agency under contract No. VEGA 1/0678/22.*

*Authors' contributions: L.B. characterized the samples with FT-IR, wrote the manuscript in consultation with P.R.; L.B. and M.S. performed the experiments; M.S. processed the experimental data; P.R. manufactured the samples and characterized them with TGA; A.P. responsible for the final editing of the manuscript in consultation with P.R. and L.B.; P.G. characterized the samples with SEM, EDX and XRD.*

### **REFERENCES**

1. M. Ahmadian, H. Derakhshankhah, M. Jaymand, Biosorptive removal of organic dyes using natural gums-based materials: A comprehensive review, *J. Ind. Eng. Chem.*, 124, 2023, 102-131.
2. M.F. Hanafi, N. Sapawe, A review on the water problem associate with organic pollutants derived from phenol, methyl orange, and remazol brilliant blue dyes, *Mater. Today Proc.*, 31, 2020, A141-A150.
3. Z. Mulushewa, W.T. Dinbore, Y. Ayele, Removal of methylene blue from textile waste water using kaolin and zeolite-x synthesized from Ethiopian kaolin, *Environ. Anal. Health. Toxicol.*, 36, 1, 2021, e2021007.
4. P.O. Oladoye, T.O. Ajiboye, E.O. Omotola, O.J. Oyewola, Methylene blue dye: Toxicity and potential elimination technology from wastewater, *Results Eng.*, 16, 2022, 100678.
5. pubchem.ncbi.nlm.nih.gov, Methylene Blue, Available 2024-01-16 at <<https://pubchem.ncbi.nlm.nih.gov/compound/Methylene-Blue#section=Synonyms>>
6. American Chemical Society, Methylene Blue. Available 2023-19-03 at <<https://www.acs.org/molecule-of-the-week/archive/m/methylene-blue.html>>
7. IARC Working Group on the Evaluation of Carcinogenic Risks to Humans, Some Drugs and Herbal Products, Lyon (FR): International Agency for Research on Cancer, 108, 2016.
8. R. Kishor, D. Purchase, G.D. Saratale, R.G. Saratale, L.F.R. Ferreira, M. Bilal, R. Chandra, R.N. Bharagava, Ecotoxicological and health concerns of persistent coloring pollutants of textile industry wastewater and treatment approaches for environmental safety, *J. Environ. Chem. Eng.*, 9, 2, 2021, 105012.
9. B. Lellis, B.C.Z. Fávoro-Polonio, J.A. Pamphile, J.C. Polonio, Effects of textile dyes on health and the environment and bioremediation potential of living organisms, *Biotechnol. Res. Innov.*, 3, 2019, 275-90.
10. I. Khan, K. Saeed, I. Zekker, B. Zhang, A.H. Hendi, A. Ahmad, S. Ahmad, N. Zada, H. Ahmad, L.A. Shah, T. Shah, I. Khan, Review on Methylene Blue: Its Properties, Uses, Toxicity and Photodegradation, *Water*, 14, 2, 242, 2022.
11. E. Bistas, D.K. Sanghavi, Methylene Blue. [Updated 2023 Jun 26]. In: StatPearls [Internet]. Treasure Island (FL): StatPearls Publishing, 2024. Available at <<https://www.ncbi.nlm.nih.gov/books/NBK557593/>>
12. E. Rápó, S. Tonk, Factors Affecting Synthetic Dye Adsorption; Desorption Studies: A Review of Results from the Last Five Years (2017-2021), *Molecules*, 26, 17, 5419, 2021.
13. S. Dutta, B. Gupta, S.K. Srivastava, A.K. Gupta, Recent advances on the removal of dyes from wastewater using various adsorbents: a critical review, *Mater. Adv.*, 2, 2021, 4977-4531.
14. ensingerplastics.com, PET - Polyethylene terephthalate. [online]. [cit. 2024-04-10], Available at <<https://www.ensingerplastics.com/en-us/shapes/engineering-plastics/pet-polyester>>
15. T.M. Joseph, S. Azat, Z. Ahmadi, O.M. Jazani, A. Esmaeili, E. Kianfar, J. Haponiuk, S. Thomas, Polyethylene terephthalate (PET) recycling: A review, *Case Stud. Chem. Environ. Eng.*, 9, 2024, 100673.
16. N.A. El Essawy, S. M. Ali, H.A. Farag, A.H. Konsowa, M. Elnouby, H.A. Hamad, Green synthesis of graphene from recycled PET bottle wastes for use in the adsorption of dyes in aqueous solution, *Ecotoxicol. Environ. Saf.*, 145, 2017, 57-68.

17. P. Dutt, Green Illusions: The Harsh Reality of PET Bottle Recycling. Available at 06/2023, <<https://www.linkedin.com/pulse/green-illusions-harsh-reality-pet-bottle-recycling-prakash-dutt/>>
18. M.N. Ezzat, Z.T.A. Ali, Green approach for fabrication of graphene from polyethylene terephthalate (PET) bottle waste as reactive material for dyes removal from aqueous solution: Batch and continuous study, *Sustain. Mater. Technol.*, 32, 2022, e00404.
19. M.S. Islam, K.N. McPhedran, S.A. Messele, Y. Liu, M.G. El-Din, Isotherm and kinetic studies on adsorption of oil sands process affected water organic compounds using granular activated carbon, *Chemosphere*, 202, 2018, 716-725.
20. Y.S. Ho, G. McKay, The kinetics of sorption of divalent metal ions onto sphagnum moss peat, *Water Res.*, 34, 2000, 735-742.
21. H. Qiu, L. Lv, B. Pan, Q. Zhang, W. Zhang, Q. Zhang, Critical Review of Adsorption Kinetic Models, *J. Zhejiang Univ. Sci.*, 10, 2009, 716-724.
22. Y.S. Ho, G. McKay, A kinetic study of dye sorption by biosorbent waste product pith, *Resour. Conserv. Recycl.*, 25, 1999, 171-193.
23. Y.S. Ho, Review of Second-Order Models for Adsorption Systems, *J. Hazard. Mater.*, 136, 2006, 681-689.
24. M. Elkady, H. Shokry, H. Hamad, Effect of superparamagnetic nanoparticles on the physicochemical properties of nano hydroxyapatite for groundwater treatment: adsorption mechanism of Fe(II) and Mn(II), *RSC Adv.*, 6, 2016, 82244-82259.
25. N.Z. Rebitanim, W.A.W.A.K. Ghani, D.K. Mahmoud, N.A. Rebitanim, M.A.M. Salleh, Adsorption Capacity of Raw Empty Fruit Bunch Biomass onto Methylene Blue Dye in Aqueous Solution, *J. Purity, Util. React. Environ.*, 1, 2012, 45-60.
26. A.P.S. Pereira, M.H.P. Silva, E.P. Lima Júnior, A.S. Paula, F.J. Tommasini, Processing and Characterization of PET Composites Reinforced With Geopolymer Concrete Waste, *Mat. Res.*, 20, 2017, 411-420.
27. M.J. Chinchillas-Chinchillas, V.M. Orozco-Carmona, C.G. Alvarado-Beltrán, J.L. Almaral-Sánchez, S. Sepulveda-Guzman, L.E. Jasso-Ramos, A. Castro-Beltrán, Synthesis of Recycled Poly(ethylene terephthalate)/Polyacrylonitrile/Styrene Composite Nanofibers by Electrospinning and Their Mechanical Properties Evaluation, *J. Polym. Environ.*, 27, 2019, 659-669.
28. S. Park, S. Thanakkasaranee, H. Shin, Y. Lee, G. Tak, J. Seo, PET/Bio-Based Terpolyester Blends with High Dimensional Thermal Stability, *Polymers*, 13, 5, 2021, 728.
29. F. Farivar, P.L. Yap, R.U. Karunagaran, D. Losic, Thermogravimetric analysis (TGA) of graphene materials: Effect of particle size of graphene, graphene oxide and graphite on thermal parameters, *C*, 7, 2, 41, 2021.
30. P.L. Yap, S. Kabiri, D.N.H. Tran, D. Losic, Multifunctional binding chemistry on modified graphene composite for selective and highly efficient adsorption of mercury, *ACS Appl. Mater. Interfaces.*, 11, 2019, 6350-6362.
31. F. Farivar, P.L. Yap, K. Hassan, T.T. Tung, D.N.H. Tran, A.J. Pollard, D. Losic, Unlocking thermogravimetric analysis (TGA) in the fight against "Fake graphene" materials, *Carbon*, 179, 2021, 505-513.
32. Y. Shen, A.Ch. Lua, A facile method for the large-scale continuous synthesis of graphene sheets using a novel catalyst, *Sci. Rep.*, 3, 3037, 2013.
33. J. Zhang, X. Wang, G. Qi, B. Li, Z. Song, H. Jiang, X. Zhang, J. Qiao, A novel N-doped porous carbon microsphere composed of hollow carbon nanospheres, *Carbon*, 96, 2016, 864-870.
34. R. Sergiienko, E. Shibata, S. Kim, T. Kinota, T. Nakamura, Nanographite structures formed during annealing of disordered carbon containing finely-dispersed carbon nanocapsules with iron carbide cores, *Carbon*, 47, 2009, 1056-1065.
35. F.T. Johra, J. W. Lee, W.-G. Jung, Facile and safe graphene preparation on solution based platform, *J. Ind. Eng. Chem.*, 20, 5, 2014, 2883-2887.
36. B. Hu, Y. Ai, J. Jin, T. Hayat, A. Alsaedi, L. Zhuang, X. Wang, Efficient elimination of organic and inorganic pollutants by biochar and biochar-based materials, *Biochar*, 2, 2020, 47-64.